Optimizing Energy Absorption for Ultrashort Pulse Laser Ablation of Fused Silica

Nicolas Sanner, Maxime Lebugle, Nadezda Varkentina, Marc Sentis and Olivier Utéza

Aix-Marseille Univ., CNRS, LP3 UMR 7341, 163 avenue de Luminy C.917, 13288 Marseille, France

Keywords: Ultrashort Laser-matter Interaction, Dielectric Materials, Ablation.

Abstract: We investigate the ultrafast absorption of fused silica irradiated by a single 500 fs laser pulse in the context of micromachining applications. As the absorption of the laser energy is rapid (~fs), the optical properties of the material evolve during the laser pulse, thereby yielding a feedback on the dynamics of absorption and consequently on the amount of energy that is absorbed. Through complete investigation of energy absorption, by combining "pump depletion" and "pump-probe" experiments in a wide range of incident fluences above the ablation threshold, we demonstrate the existence of an optimal fluence range, enabling to turn transiently the material into a state such that each photon is optimally utilized for ablation.

1 INTRODUCTION

Ultrashort laser pulses are extremely interesting and powerful tools for laser-matter interaction. The spatial accuracy of energy deposition into matter combined with the shortness of the energy deposition step enable to reach relatively high intensities (10^{13}-10^{14} W.cm^{-2}) while using low energies, capable to push matter into strongly non-equilibrium conditions (Gamaly, 2011). The fast creation of highly excited plasmas at solid densities provides notably cutting-edge capabilities for controlled modification of matter. Near-IR wavelengths of most current femtosecond laser sources are particularly well adapted to trigger highly-nonlinear absorption in transparent dielectric materials (silica, sapphire, diamond…), whose range of applications for material science and photonics is extremely extended.

First, the possibility to rapidly transform such insulating materials into plasmas within 10^{-15} second timescale and on micrometric dimensions is of strong interest for a vast panel of future ultrafast applications (Sugioka and Cheng, 2013): change of electrical properties for ultrafast laser-induced electronic switches, change of optical properties for ultrafast plasma mirrors and plasma optics, structural change of atomic lattice (ultrafast melting) enabling to change the refractive index, etc. Second, for intensities above the material ablation threshold, the final result is highly interesting for material processing at micro- and nano-scales: voids for memories, channels for microfluidic, ophthalmic/neuronal surgery, material cutting, drilling, surface structuration (e.g. for metamaterials or plasmonics), etc. All these cutting-edge applications for future technology and industry are based on ultrafast laser-induced ionization of dielectric solids, which provides time- and space-confinement of energy for matter transformation.

Even for ablation, for which several temporal orders of magnitude separate the very first stage of interaction (ionization) and the removal of matter produced by one single pulse, experimental observations establish that the result of ablation is closely linked to and driven by the mechanisms and the dynamics of absorption (Balling and Schou, 2013). Yet, it turns out that for material ablation, the total amount of energy that is deposited in the material is of highest importance, since part of the interacting energy is not optimally used for ablation and is finally relaxed into unwanted effects in the material (recast products, rims, thermal load, residual mechanical constraints, etc.) (Ben-Yakar et al., 2007). Although these effects are reduced in the femtosecond pulse regime compared to longer pulse durations, they are nevertheless no more negligible when dealing with the micrometer scale. For the best control of the outcome of ablation, it is therefore important to provide no more than the amount of laser energy necessary to machine the calibrated modification of the material surface.

In this context, it is important to precisely know the response of the material, both temporally and under various intensities of irradiation, to optimize the result of ablation. Dielectric materials being initially transparent to near infrared laser light, non-linear absorption mechanisms are required to bridge the band gap and promote free electrons in the conduction band (Stuart et al., 1996). These seed electrons are further accelerated through inverse Bremsstrahlung (IB) and multiplied by impact ionization (II) if their kinetic energy is sufficient, leading to an avalanche multiplication phenomenon. Strong laser absorption therefore takes place in the first (hundred) nanometers at the surface of the material, where the material has been turned opaque. It may yield to damage or ablation of the material, if the quantity of laser energy absorbed by the material is sufficiently high and properly adjusted (Jia et al., 2004, Chimier et al., 2011). At densities higher than the critical plasma density, the material optical properties evolve during the laser pulse, thereby yielding a feedback on the dynamics of absorption (Chowdhury et al., 2005, Hernandez-Rueda et al., 2012) and consequently on the amount of energy that is absorbed. This actually depends on the characteristics of the plasma layer which is created at the surface of the sample by the pulse itself.

To explore this, we present here a complete investigation of energy absorption, by combining "pump-probe" (Lebugle et al., 2014) and "pump depletion" (Varkentina et al., 2013) experiments in a wide range of incident fluences above the ablation threshold. The first offers the ability to follow in time the free-electrons plasma buildup and its transient optical properties, while the latter provides information concerning the absorbed energy. This extensive information finally provides a comprehensive picture of material response and strategies for optimizing the amount of energy that is eventually deposited in the material.

2 DYNAMICS OF ABSORPTION

2.1 Setup and Determination of Time Zero

In order to probe the absorption *during* the irradiating pulse, and therefore provide insights into the mechanisms and dynamics of absorption, two main conditions must be fulfilled (Lebugle et al., 2015):

(i) Use a probe pulse much shorter than the pump, to obtain high temporal sampling

(ii) Accurately determine the 'time zero', i.e. the zero-delay instant between the peaks of the pump and the probe pulses.

To address the first condition, we use a 500-fs pump pulse, delivered by a commercial source (emitting at 1025 nm) and a 60-fs probe pulse at the same wavelength, issued from self-phase modulation in a microstructured fiber and further compressed by chirped mirrors. The probe pulse duration is therefore a factor of eight shorter than the pump pulse, thus allowing accurate temporal sampling of the optical transient states. The experimental setup is sketched in Figure 1. The pump beam is focused with normal incidence at the surface of the SiO_2 sample with horizontal polarization, and probed by the s-polarized pulse at an angle of 20°. The two beams are carefully mode-matched, with radii of ~13 μm at $1/e^2$ in intensity, measured by imaging of the beams onto a CCD camera with adapted magnification. The reflected and transmitted parts of the probe pulse are recorded by photodiodes after spectral, spatial (lens and pinhole) and polarization filtering.

The second condition is of highest importance to retrieve the exact temporal dynamics of mechanisms involved in the interaction at the timescale of the pulse. Instead of using nonlinear crystal in place of the SiO_2 sample to perform SHG or THG for determining the 'time zero', we directly rely on the nonlinear second order coefficient of fused silica itself ($n_2 \approx 3 \times 10^{-7} cm^2/GW$). This offers the advantage to work directly in-situ, and suppresses the difficulty to further position the surface of the target material exactly in the same plane as the non-linear crystal used once it has been removed. This configuration is in fact a polarization-gated cross-correlation FROG experiment (PG-XFROG). It enables to characterize in situ the probe pulse (intensity and phase), but more importantly to accurately calibrate the temporal overlap between the pump and probe pulses. For that, the polarization of the pump pulse is set to be 45° with respect to that of the probe one, and the photodiode monitoring the p-component of the polarization of the probe pulse is also replaced by a spectrometer. Upon irradiation by a low-energy pump pulse, transient birefringence appears inside the fused silica sample during the pump pulse, so that the polarization of the probe beam is slightly turned to allow spectral analysis by the spectrometer of the signal coming through the p-transmitting polarizing beam-splitter. By time delaying the probe pulse with respect to the pump pulse, the spectrally resolved PG-XFROG signal is recorded. We finally retrieve the probe pulse

duration of 60 fs, in excellent agreement with independent measurement performed with a second-order autocorrelator. More importantly, the zero-time delay is defined by the instant of superposition of the peaks of the pump and probe pulses, with a precision of ± 30 fs.
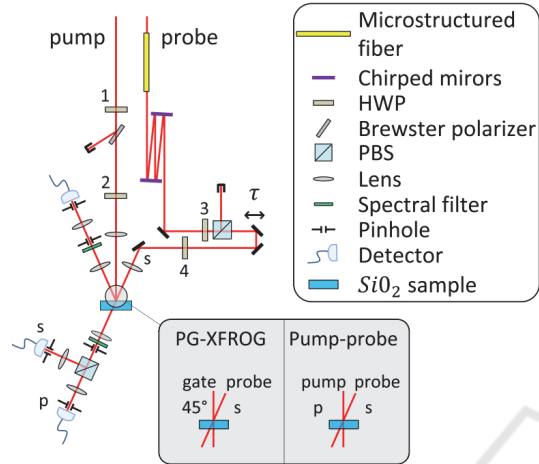

Figure 1: Experimental set-up. A 500-fs pulse is split into two arms, and the probe pulse is further compressed down to 60 fs using spectral broadening in a micro-structured fibre, with the second-order spectral phase adjusted with a pair of chirped mirrors. The two pulses are then focused on the surface of the fused silica target, controlling the delay between them. This pump–probe set-up, which is designed to measure the optical dynamics during laser excitation, makes also possible the direct calibration of the time zero in a PG-XFROG configuration as well as measuring the probe pulse (intensity and phase), provided that the polarizations are properly set (see insets).

2.2 Dynamics of Transient Absorption

Now turning back to pump-probe experimental configuration, transient optical properties of the fused silica sample that transforms into plasma during the pump pulse are measured as a function of time delay for a set of increasing fluences. Note that these experiments are performed in single pulse regime. Moreover, although the peak powers attained with the highest fluences used here (~60 MW) largely exceed the critical power for self-focusing in the fused silica sample (~3 MW at this wavelength), in our experiments we do not detect any signs of sub-surface or bulk laser-induced damage.

For pump fluences below the ablation threshold $F_{th} \approx 5.8 \, J/cm^2$, no significant variations of the probe signals are recorded, whereas for all fluences higher than the ablation threshold the plasma properties strongly evolve during the pulse. Note

that we use a low-intensity probe pulse, whose intensity ($I_{probe} \approx 2 \times 10^{11} W/cm^2$) is well below any material modification threshold for a 60 fs pulse. Indeed, we verified that no depletion of the probe pulse occurs when the pump beam is blocked. We also experimentally checked that no change is observable in the response of the plasma as a function of the probe energy. Thus, the plasma absorption read by the probe mainly corresponds to absorption by IB, i.e. the heating of the free carriers (produced by the pump pulse) through collisions of a photon with an electron in the field of the parent atom. The magnitude of this one-photon absorption of the probe is then directly representative of the free electron density of the plasma.

Transient transmissivity T and reflectivity R recorded during the pulse are shown in Figure 2. A large set of fluences is explored, from $0.7F_{th}$ to $3.9F_{th}$. All the curves show absolute values, so that their initial values measured before the pump pulse account for Fresnel reflection. With these measurements, absorptivity can be deduced using the energy conservation law: $A = 1 - R - T$.

Temporally, the curves present swift changes in the second half of the pump pulse. They saturate after the pulse at a time delay around 0.5 ps for all fluences. Concerning the reflectivity R, we observe that a plasma mirror effect occurs during the pulse, and therefore partially limits energy deposition. This evidences the formation of a transient overdense plasma during the excitation pulse.

Now concerning absorption and its transient dynamics, instantaneous absorption is maximal at the end of the pulse (delay of ~500 fs). Transient plasma absorption is higher and starts earlier (before pump maximum) for growing fluences. At this point, it is important to recall that what is measured is the absorption of the probe pulse by Inverse Bremsstrahlung (IB) at 1025 nm, meaning that the probe pulse "reads" the plasma absorption properties. Yet, since the probe and pump pulses have the same wavelength and same spot size, this demonstrates that IB absorption of the pump pulse itself has a growing contribution during the second half of the pulse, beginning earlier and earlier upon increase of the fluence. The magnitude of IB absorption reaches 40% for the highest fluence $3.9F_{th}$, which is an indication that the predominant mechanism of pump absorption is impact ionization. However, we must remind that this is a mean value, averaged on the whole spatial extend of the 2D Gaussian beam profile. Thus, this effect should be much more pronounced at the center of the beam.

Finally, these combined observations of R and T

suggest the existence of a fluence range that may enable to maximize the transfer of energy from the laser pulse to the material. Ideally, overall reflectivity should keep moderate, together with high level of absorption. In this perspective, it is interesting to point out the saturation of absorptivity when fluence increases. Indeed, only a small variation is recorded between the curves for $2.5F_{th}$ and $3.9F_{th}$. This is analyzed with respect to integrated measurements in the next section, in order to identify the optimal fluence range for ablation.
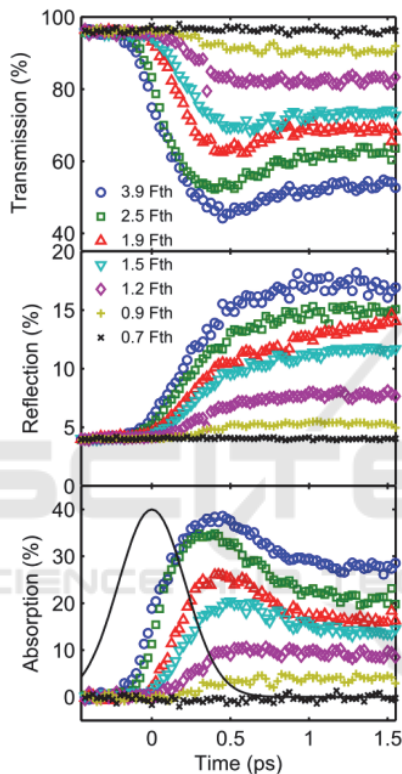

Figure 2: Transient optical properties of the fused silica sample during the pulse (retrieved from pump-probe experiments). Each data point is the average of 5 independent measurements. The pump pulse is also represented with a Gaussian function of 500 fs duration FWHM (arbitrary vertical units).

3 EFFICIENCY OF ABSORPTION FOR ABLATION

With the aim to link absorption with ablation, we also implemented a "pump-depletion" experiment. In a complementary manner with the pump-probe experiment, we thus explore the total absorption of the pump beam, temporally integrated over the whole pulse length.

This setup uses the same kind of experimental arrangement as presented in Figure 1, but only the pump pulse is present. The same incident laser beam is focused on the sample surface, but here the beam radius is smaller than in the previously presented experiment (6.3 µm at $1/e^2$). However, the measured fluence for ablation threshold is identical, making therefore possible to compare directly these two experiments. The transmitted and reflected fractions of the incident pump pulse are measured with proper photodiodes and filtering. Note that here these signals are integrated both spatially (over the radially Gaussian beam distribution) and temporally (over the whole pulse length).

Post-mortem analyses of the ablated craters are performed by atomic force microscopy, and we define the absorption efficiency η_{abs} as the ratio of the ablated volume V to the absorbed pulse energy: $\eta_{abs} = V/E_{abs}$. Note that this quantity is different from the usual ablation efficiency used in other works (Utéza et al., 2011) based on incident rather than absorbed energy. Figure 3 shows that the laser energy is more and more efficiently absorbed for growing fluences, until the curve reaches a plateau (~ 0.65 µm³/µJ) followed by a slow decrease. This saturation appears for fluences that are well in accordance with the saturation of absorption measured in the in the previous section, i.e. for fluences around three times the ablation threshold.

A fluence range $\Delta F_{eff,abs}$ corresponding to efficient absorption for ablation can be interestingly identified. Its limits are defined with respect to the fluences yielding ~90% of the maximum absorption efficiency. According to that criterion, the absorption is efficient from ~2 to $\sim 8F_{th}$. It is important to determine the range of $\Delta F_{eff,abs}$ when one is intended to develop micromachining applications. Indeed, it helps to define an optimal working fluence range, where maximal absorption is attained and the energy deposition is not too strongly disturbed by the plasma screening effect. From the viewpoint of efficient material removal, reaching this precise state of the material optimizes absorption efficiency, i.e. enables the optimal utilization of photons for material ablation.

Moreover, the best ablation quality is also obtained for fluence values corresponding to the $\Delta F_{eff,abs}$ range, as illustrated by the typical crater morphology displayed on figure 3 (corresponding to $3.9F_{th}$). Below $2F_{th}$, the energy is not sufficient to produce a smooth ablation (high surface roughness), and above $8F_{th}$ we observe a higher level of debris and a lower efficiency removal, which is often not suitable for applications.
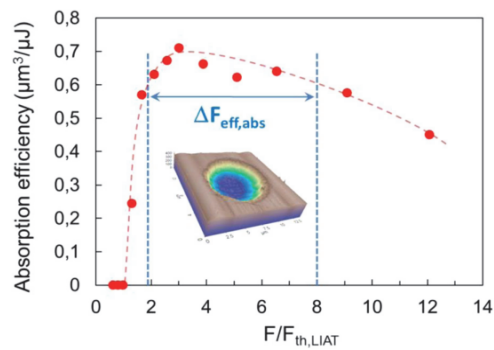
Figure 3: Absorption efficiency $\eta_{abs} = V/E_{abs}$, as a function of normalized laser fluence. $\Delta F_{eff,abs}$ determines a fluence zone of high efficiency of absorption, by taking a criterion of 90% of the maximum value. For illustration, an AFM picture of a typical crater obtained in this range is shown (corresponding here to $3.9F_{th}$, with a crater diameter of 9.3 µm and a maximum depth of 210 nm).

4 CONCLUSIONS

In conclusion, the dynamics of transient optical properties of silica during a 500-fs laser pulse is retrieved and compared to time-integrated ones, obtained by independent energy balance measurement. The high temporal resolution achieved in this experiment enables to reveal the fine dynamics of transient material states. In particular, for ablation purposes, it appears that an optimal fluence range (with respect to ablation efficiency) is identified between two and four times the ablation threshold. This corresponds to a very particular situation: the material has already turned strongly absorbing, whereas its reflective properties are still low. This is taking place mostly in the second half of the pulse. In this regime, the incident laser energy is best absorbed.

By demonstrating that a careful choice of the incident fluence promotes a large coupling of the incoming laser energy to the excited material, this work is of particular importance in the context of micromachining process, for which a better control of the material excitation is sought. Our results highlight the crucial role of transient optical properties during the laser-matter interaction in the regime of ablation, and open a comprehensive way toward designing dedicated user-defined temporal excitation profiles.

ACKNOWLEDGEMENTS

REFERENCES

Gamaly, E., 2011. *Femtosecond laser-matter interactions.* Pan Stanford Publishing.

Sugioka, K., Cheng, Y., 2013. *Ultrafast Laser Processing: From Micro- to Nanoscale*, Pan Stanford Publishing.

Balling, P., Schou, J., 2013. Femtosecond-laser ablation dynamics of dielectrics: basics and applications for thin films. *Rep. Prog. Phys.* 76 036502.

Ben-Yakar, A., Harkin, A., Ashmore, J., Byer, R.L., Stone, H.A., 2007. Thermal and fluid processes of a thin melt zone during femtosecond laser ablation of glass: the formation of rims by single laser pulses. *J. Phys. D: Appl. Phys.* 40 1447–1459.

Stuart, B.C., Feit, M.D., Herman, S., Rubenchik, A.M., Shore, B.W., and Perry, M.D., 1996. Nanosecond-to-femtosecond laser-induced breakdown in dielectrics. *Phys. Rev. B* 53, 1749.

Jia, T., Xu, Z., Li, R., Feng, D., Li, X., Cheng, C., Sun, H., Xu, N., and Wang, H., 2004. Mechanisms in fs-laser ablation in fused silica *J. Appl. Phys.* 95(9), 5166.

Chimier, B., Utéza, O., Sanner, N., Sentis, M., Itina, T., Lassonde, P., Légaré, F., Vidal, F. and Kieffer, J.C.. 2011. Damage and ablation thresholds of fused-silica in femtosecond regime *Phys. Rev. B* 84, 094104.

Chowdhury, I.H., Wu, A.Q., Xu, X., and Weiner, A.M. 2005. Ultra-fast laser absorption and ablation dynamics in wide-band-gap dielectrics *Appl. Phys. A* 81, 1627.

Hernandez-Rueda, J., Puerto, D., Siegel, J., Galvan-Sosa, M., and Solis, J. 2012 Plasma dynamics and structural modifications induced by femtosecond laser pulses in quartz *Appl. Surf. Sci.* 258(23), 9389.

Lebugle, M., Sanner, N., Varkentina, N., Sentis, M., and Utéza, O. 2014 Dynamics of femtosecond laser absorption of fused silica in the ablation regime *J. Appl. Phys.* 116, 063105.

Varkentina, N., Sanner, N., Lebugle, M., Sentis, M., and Utéza, O. 2013 Absorption of a single 500fs laser pulse at the surface of fused silica: Energy balance and ablation efficiency *J. Appl. Phys.* 114, 173105.

Lebugle, M., Utéza, O., Sentis, M., and Sanner, N. 2015 High temporal resolution and calibration in pump–probe experiments characterizing femtosecond laser–dielectrics interaction, *Appl. Phys. A* 120, 455–461.

Utéza, O., Sanner, N., Chimier, B., Brocas, A., Varkentina, N., Sentis, M., Lassonde, P., Légaré, F. and Kieffer. 2011 Control of material removal of fused silica with single pulses of few optical cycles to sub-picosecond duration *Appl. Phys. A* 105, 131.